Biomedical Signals & Systems Research Group

Faculty of Electrical Engineering, Mathematics and Computer Science

Effect of Running Speed on Lower Leg Muscle Activation and Tibial Bone Load

Bridging External Measurements and Internal Load Dynamics

Thesis - MSc. Biomedical Engineering

Sietse de Koning

Graduation Committee:
Dr. J. Reenalda
Dr. Ir. B.L. Scheltinga
Prof. Dr. Ir. M. Sartori

Date:
May 30, 2025

UNIVERSITY OF TWENTE.

Contents

1 Introduction **2**

2 Method **4**
- 2.1 Participants 4
- 2.2 Measurement systems 4
- 2.3 Measurement protocol 5
- 2.4 Data Processing 5
  - 2.4.1 IMU data 5
  - 2.4.2 Motion Capture data 6
  - 2.4.3 Force-Plate data 6
  - 2.4.4 EMG data 6
  - 2.4.5 Temporal synchronization 6
- 2.5 Statistical Analysis 6

3 Results **7**
- 3.1 Tibial Bone Load and Muscle Activations During the Swing and Stance Phases 7
- 3.2 Effect of Running Speed on Peak Force Magnitudes 7
- 3.3 Ratio of Peak Internal Muscle Forces to External Impact Forces at various Speeds 8
- 3.4 Effect of Running Speed on Peak Muscle Activation Magnitudes 8
- 3.5 Timing of Peak Forces and Peak Activations 8

4 Discussion **8**

5 Conclusion **10**

6 Acknowledgements **10**

Abstract

Running is a very popular sport, but it is also associated with a high incidence of lower extremity overuse injuries, with the tibia being the most commonly affected location. Gaining insight into tibial loading and its underlying contributors, such as muscle activation, can improve our understanding of the origins behind these injuries and support the development of effective prevention and intervention strategies. This study investigated the effect of running speed on tibial loading and muscle activation of the tibialis anterior, soleus, gastrocnemius medialis, and gastrocnemius lateralis during the stance and swing phases.

Nine subjects ran intervals at four different speeds (8, 10, 12, and 14 km/h) on a force plate-instrumented treadmill, while data were simultaneously collected using a motion capture system, inertial measurement units (IMUs), and EMG electrodes.

Statiscal analysis using Linear Mixed Models (LMMs) showed that, internal muscle forces, external impact forces, and total tibial bone load (TBL) increased significantly ($p < 0.005$) with speed. For every 1 km/h increase, peak internal force rose by 0.156 ± 0.011 BW, external force by 0.050 ± 0.005 BW, and total TBL by 0.192 ± 0.016 BW. The ratio between internal and external forces increased with speed, while peak timing remained unaffected.

Muscle activation increased significantly ($p < 0.005$) with running speed for all measured muscles. For every 1 km/h increase in speed, tibialis anterior activation increased by 0.107 ± 0.011, soleus by 0.059 ± 0.009, gastrocnemius lateralis by 0.101 ± 0.011, and gastrocnemius medialis by 0.041 ± 0.008. This indicates that the tibialis anterior and gastrocnemius lateralis showed the largest relative increases, while the soleus and gastrocnemius medialis exhibited more moderate changes.

Because internal muscle force and external impact force increase at different rates with running speed, their ratio is speed-dependent and shows an increase of 0.028 ± 0.006 per 1 km/h. This ratio could be used to estimate internal muscle forces alongside estimated external impact forces from wearable sensors, enabling an overall estimation of total tibial loading. Such an approach may facilitate easier and more accessible monitoring of loading in real-world settings and improve research into overuse injuries.

1 Introduction

Running is a widely practiced physical activity that offers numerous health benefits [1]. Unfortunately, injuries are quite prevalent among runners. The exact incidence varies among the studied subgroups, and which definition of a running injury is used [2, 3]. In their systematic review, van Gent et al. (2007) reported a range of incidences of lower extremity running injuries, varying from 19.4% to 79.3%[2]. Bone stress fractures contribute to approximately 6% to 14% of the injuries occurring in runners [4, 5, 6]. Stress fractures are often attributed to recurring impact or strenuous physical activity, with insufficient opportunity for the bone to properly recover [7, 8]. The tibia is the most susceptible bone for stress fractures and represents a significant proportion of the stress fractures, ranging between 20% and 56%, of all cases [7, 9, 10, 11].

Mechanical loading of the tibia, referred to as *Tibial Bone Load* (TBL) in this study, is assumed to be a key factor contributing to the development of tibial stress fractures [4, 6, 12]. Consequently, numerous studies have aimed to quantify TBL during running [13]. Direct measurements of TBL are only feasible following invasive surgery involving in vivo force sensor placement [6, 14, 15], complicating research into the mechanical loading of running. Therefore, alternative measures have been used to assess the mechanical load on the tibia. Examples of loading surrogates or proxies are *Ground Reaction Forces* (GRF), which represent the force exerted by the ground on the body during foot contact, and *Peak Tibial Acceleration* (PTA), which reflects the maximum acceleration of the tibia at foot strike. Multiple studies have found correlations between GRF and tibial bone stress fractures [16, 17], as well as between PTA and tibial bone stress fractures [18, 19]. However, this association is only evident at the group level, as there is strong variation among individuals [20, 21]. These findings challenge the assumption that such surrogates or proxies reliably reflect TBL in individual runners.

Matijevich et al. (2019) demonstrated, using a Sagittal Plane Ankle Model, that GRF should not be assumed to correlate with the TBL [21]. Similarly, the study by Zandbergen et al. (2023) demonstrated that PTA is not a reliable indicator of TBL for individual runners, given the low and non-significant correlation between PTA and TBL [22].

The sagittal plane ankle model used by Matijevich (2019) and Zandbergen (2023) originates from earlier scientific work by Scott & Winter (1990) [21, 22, 23, 24], and describes the tibial compression force (F_{tibia}) as the sum of the external impact force (F_{ext}) and internal muscle force (F_{int}), which together determine the total load on the tibia. This can be expresses as:

$$F_{tibia}(t) = F_{int}(t) + F_{ext}(t)$$

External impact forces are generated by the interaction between the foot and the ground, as the body's weight, due to gravity, acts on the foot during ground contact. These forces are typically represented by GRF measurements, often obtained using force plates, which can also be integrated into a treadmill.

Internal muscle forces arise from muscular contractions required for movement and stabilization.

The primary muscles contributing to sagittal plane ankle movement during running are the soleus, the gastrocnemius medialis and lateralis, and the tibialis anterior [25]. The soleus and gastrocnemius muscles are responsible for plantar flexion and generate the force needed to push off [25, 26]. The force generated by the muscles is directed through the achilles tendon to which the muscles are distally attached [26]. The medial head of the gastrocnemius finds its origin at the posterior side of the medial femoral condyle, the lateral head of the gastrocnemius finds its origin at the posterior side of the medial femoral condyle, making it a bi-articular muscle [27]. The soleus originates at the proximal posterior tibia, the fibula, and the interosseous membrane [27]. The tibialis anterior is responsible for dorsiflexion and stabilization of the ankle during foot strike and swing phase [26, 28]. The tibialis anterior originates at the lateral condyle of the tibia and is inserted at the medial cuneiform bone [28]. Other muscles, such as tibialis posterior, flexor digitorum longus, and flexor hallucis longus, as well as the peroneal muscle group (peroneus longus and peroneus brevis), contribute to fine motor control and stabilization of the foot and ankle. However, because their estimated contribution to tibial loading is relatively small, proximately less than 10%, these muscles were therefore not considered in this study [25].

In the model, the external impact force acting on the tibia is estimated by projecting the resultant GRF onto the longitudinal axis of the tibia. This is done by multiplying the magnitude of the absolute GRF vector with the cosine of the angle $\beta(t)$ between the GRF direction and the tibial axis. The resulting expression for the external impact force is:

$$F_{ext}(t) = \left|\overrightarrow{GRF}(t)\right| \cdot cos(\beta(t))$$

The internal muscle force is estimated by first calculating the ankle joint moment (M_{ankle}). This moment is obtained by multiplying the horizontal distance between the *Center of Pressure* (CoP) and the center of the ankle joint with the magnitude of the GRF in the vertical direction. To estimate the force transmitted through the Achilles tendon, this joint moment is then divided by the Achilles tendon moment arm length (r_{at}), which represents the anterior-posterior distance from the tendon's insertion on the calcaneus to the ankle joint center. In the studies by Matijevich et al. (2019) and Zandbergen et al. (2023), this moment arm was kept constant at 0.05 m [21, 22]. This results in the following equation:

$$F_{int} = \frac{M_{ankle}}{r_{at}} = \frac{GRF_z \cdot COP_{ankle,x}}{r_{at}}$$

$$F_{int} = \frac{GRF_z \cdot COP_{ankle,x}}{0.05}$$

The model only accounts for the net ankle moment, which results in plantarflexion during the stance phase. However, dorsiflexors and other stabilizing muscles, including those operating outside the sagittal plane, are also active during running [23, 22, 29, 30]. Finally, the mass and inertia of the foot are also neglected in the model [23, 22, 29, 30].

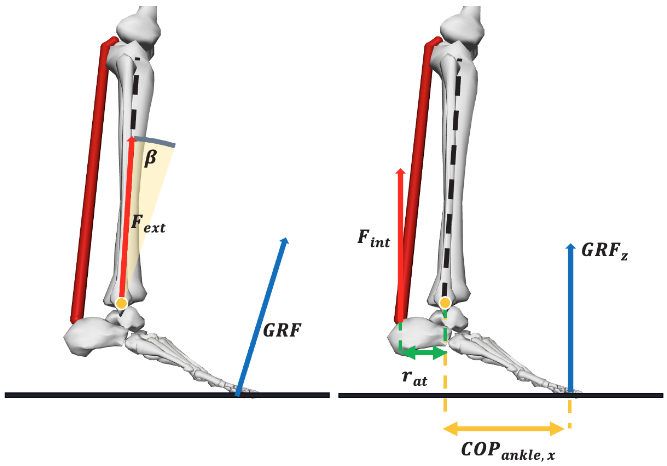

Figure 1: *On the left, the direction and point of application of the external impact force (F_{ext}) is shown, along with the parameters used to calculate this force. On the right, the direction and point of application of the internal muscle force (F_{int}) are shown, along with the parameters used to calculate this force.*

The limitations of the model are expected to lead to an underestimation of internal muscle forces. When comparing the results from studies by Matijevich et al. (2019) and Zandbergen et al. (2023) with findings from more advanced musculoskeletal models, for instance those that estimate forces using static optimization methods, notable discrepancies emerge. Internal muscle forces of 5.3 and 5.5 times body weight (BW) at a running speed of 12 km/h were reported by Matijevich et al. (2019) and Zandbergen et al. (2023), respectively [21, 22]. These values closely align with those of Kernozek et al. (2017), who observed forces of 5.5 BW at speeds ranging from 12.6 to 14.0 km/h [31]. In contrast, Sasimontonkul et al. (2007) reported substantially higher forces of 7.2 BW for a speed range of 12.6 to 14.4 km/h [25]. External impact forces reported by Zandbergen et al. (2023) and Matijevich et al. (2019), with values of 2.0 and 2.4 BW, are consistent with values reported in the literature [21, 22, 25]. To further evaluate the model's validity in estimating internal muscle forces, an alternative approach is required.
As previously stated, internal muscle force results from contractions of the lower leg muscles. By analyzing activation patterns of the muscles surrounding the ankle joint, we can gain deeper insights into the physiological drivers behind internal muscle forces. Combining muscle activation data with internal force estimates allows for a more comprehensive evaluation of the model's completeness, particularly in identifying co-contraction patterns, and enhances understanding of neuromuscular control strategies during running.
A notable challenge when comparing internal muscle force values across different studies is the variation in running speeds used in each study [21, 22, 31, 25]. Since the influence of running speed on internal muscle force remains unclear, these differences complicate cross-study comparisons. A better understanding of how running speed affects internal muscle force, external impact force and total TBL, would improve the comparability of existing findings and help determine whether observed differences are due to speed variations rather than model

discrepancies.

Moreover, understanding how running speed influences internal muscle force, external impact force, total TBL, and the activation dynamics of the muscles surrounding the ankle joint offers several potential benefits. First, insight into the relationship between running speed and tibial loading is essential for developing effective training protocols and may help reduce the risk of overuse injuries. Second, examining how the ratio between internal muscle force and external impact force changes with speed could provide a valuable metric for approximating internal loading in settings where only minimal sensor setups are available.

Recent advancements in wearable sensor technology have significantly improved the feasibility of estimating biomechanical loading outside of controlled laboratory environments [32]. Traditional gait analysis methods, such as force plates and optical motion capture, are often impractical for use in real-world or outdoor contexts. However, recent studies have demonstrated that external impact forces can be reliably estimated using minimal sensor configurations combined with machine learning techniques [33]. For example, Scheltinga et al. (2013) showed that 3D ground reaction forces can be accurately predicted using only three inertial measurement units (IMUs), highlighting the potential for real-world monitoring of external load [34].

In contrast, estimating internal muscle forces with minimal sensor setups remains a significant challenge [21, 22]. While GPS devices in combination with other wearable sensors can provide reliable data on running speed and external loading, internal loading typically requires lab-based measurements [35]. Understanding how the ratio between internal and external forces changes with speed could therefore offer a potential proxy for estimating internal loading under field conditions. This may serve as a useful direction for future research into long-term, real-world monitoring of TBL.

This study aims to explore how running speed influences total TBL and its two primary components: internal muscle force and external impact force. Special attention is given to the relative contribution of each component across different speeds. Additionally, we examine activation patterns of the muscles most responsible for internal muscles forces on the tibia.

To contribute to this broader understanding, the present study investigates how running speed influences total TBL and its two main components: internal muscle force and external impact force. In doing so, particular attention is given to how their relative contributions change with speed. Additionally, we examine the activation patterns of the muscles most responsible for internal ankle joint loading. This provides further insight into how individual muscle contributions evolve with speed, offering a more critical evaluation of the model's limitations—particularly regarding co-contraction.

2 Method

2.1 Participants

For this study, 11 healthy runners were recruited. The inclusion criteria were: (1) running at least twice per week on average over the past six months, (2) running at least eight kilometers per week on average over the past six months, (3) no major running injuries in the past six months, (4) exhibiting a rear-foot striking pattern, and (5) the ability to run at 14 km/h for at least 90 seconds.

Of the 11 participants, one was excluded after being identified as a forefoot striker during the experiment, and another's data was found to be unusable due to technical issues, resulting in nine valid measurements.

All participants were informed about the nature and purpose of the study and provided written informed consent. The study was approved by the Ethics Committee of the Faculty of Computer Science & Information Technology at the University of Twente, under reference number 24085.

2.2 Measurement systems

As part of the experimental setup, one belt of a dual-belt treadmill (Fully Instrumented Treadmill v5 [FIT5], Bertec, United States) was used. The treadmill was capable of measuring 3D GRFs and CoP, which were measured at a frequency of approximately 1000 Hz[1]. To determine the ankle kinematics, necessary for calculating the ankle joint moment arm, a marker-based motion capture system was used (Oqus Motion Capture System, Qualisys AB, Sweden), with four markers placed on each foot at the medial malleolus, lateral malleolus, toes, and calcaneus. The motion capture data was measured at 240 Hz. To measure lower body kinemetics, eight inertial measurement units were placed on the lower body and torso (Xsens MVN Link, Movella, Enschede, the Netherlands), including the feet, lower legs, upper legs, pelvis, and sternum, with data sampled at 240 Hz. Muscle activity was measured by placing EMG electrodes on the tibialis anterior, soleus, gastrocnemius medialis, and gastrocnemius lateralis, according to SENIAM guidelines [36]. The reference electrode was placed on the processus spinosus of C7. EMG was measured at 2048 Hz (Porti 7, TMSI, Oldenzaal, the Netherlands). A visual representation of the experimental setup can be seen in Figure 2.

[1] The force-plate data was measured at frequencies of 964, 1000, 1020 and 1205 Hz due to technical reasons.

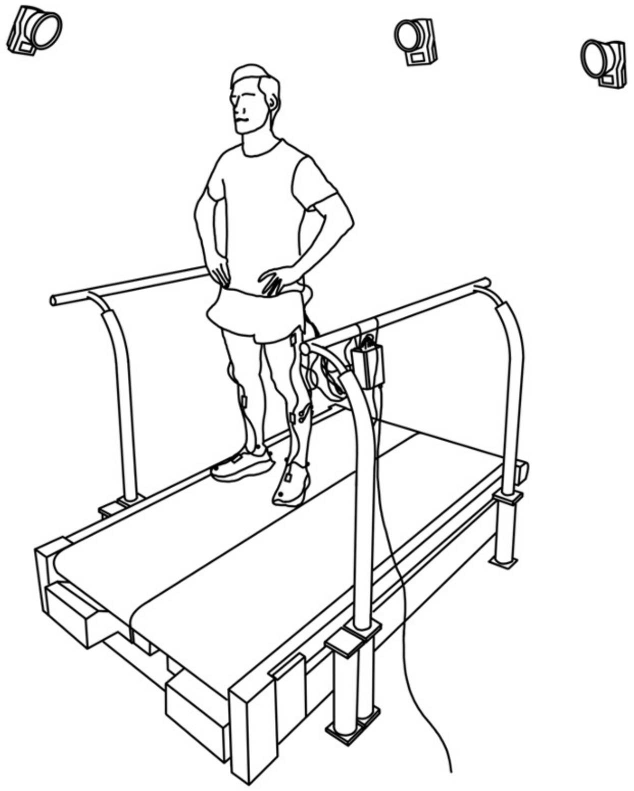

__Figure 2:__ Experimental setup with instrumented treadmill, motion capture cameras, foot markers, IMUs, and EMG electrodes. The EMG measurement device was mounted on the left handrail and the right handrail was faced outside to allow space for the runner.

2.3 Measurement protocol

Before the participant arrived, the gait laboratory was prepared and the motion capture system was calibrated. After arrival and introduction to the participant, several anthropometric measurements were taken. The recorded body measurements included body height, ankle height, knee height, hip height, hip width, shoulder height, shoulder width, elbow span, wrist span, hand span, shoe length and shoe sole thickness. Next, the IMUs were attached using double-sided tape, followed by an additional layer of elastic tape to ensure a secure fit. Next, the EMG electrodes were placed on the respective muscles, along with the reference electrode. In addition to the EMG electrodes, an accelerometer compatible with the EMG device was attached on top of the IMU sensor for the left upper leg. This was done for temporal synchronization of the IMU and EMG data. Finally, the reflective markers were placed. After all the sensors and markers were attached, body weight was measured, and the IMU sensor-to-segment calibration was carried out in accordance with the manufacturer's guidelines. The force plate was then calibrated by resetting its baseline under unloaded conditions.
After the preparation of the participants and performing the calibrations, participants were asked to warm up for five minutes by running on the treadmill at a self-selected speed. This was followed by four minutes of rest. Then, participants were asked to perform four 90-second intervals at running speeds of 8, 10, 12, and 14 km/h, with a two-minute rest period between each interval. The order of these running speeds was randomly determined to cancel out the effects of fatigue across different participants. After four minutes of rest, participants were asked to repeat the four intervals, but in a new random order, again with two-minute rest periods between the intervals. This was done to ensure that usable data would be available in case any issues occurred during the measurements. Finally, after another four-minute rest, a five-minute cool-down was performed at a speed of the participant's chose. At the start and end of every measurement, participants were asked to perform three jumps for temporal synchronization purposes.

2.4 Data Processing

To integrate and analyze the datasets originating from various measurements devices, a custom-made Python script was developed. The script was executed using Python v3.10.4 and relied on the following libraries: pandas (v1.5.3), numpy (v1.24.3), plotly (v5.14.1), matplotlib (v3.10.0), and scipy (v1.10.1).
Additionally, the TMSi-provided Python packages were used to import the EMG signals. For processing the IMU data, previously written (non-public) Python functions were utilized. The data analysis pipeline consisted of two main components. The first component was designed to filter signals from different sources, synchronize them in time, and segment relevant intervals from the recordings. For each interval, a CSV file containing the preprocessed data was generated.
The second component of the pipeline processed the data from these CSV files by dividing each measurement interval into individual steps. Using the sagittal plane ankle model, the internal muscle forces, external impact forces, and total tibial bone load (TBL) were then calculated for each step. Finally, the outcomes were averaged at two hierarchical levels: first within each participant (i.e., across their steps), and then across all participants, to enable further (statistical) analysis.

2.4.1 IMU data

The initial processing of the IMU data was performed using the Xsens MVN Analyze software (V2021.0) provided by the IMU sensor manufacturer (Xsens MVN Analyze, Movella, Enschede, the Netherlands). This software used sensor orientations in combination with subject-specific anthropometric measurements to create a scaled biomechanical model of each participant. Based on this model, kinematics and 3D joint center coordinates of the lower body were computed.
The orientation of the global IMU-based coordinate system was determined during the sensor-to-segment calibration, which meant that the system's X-axis did not always align with the actual running direction of the participant. However, because the software estimated the participant's displacement, even during treadmill running, it was possible to reorient the coordinate system based on the running direction observed in the transverse plane.
As the MVN software already applied filtering methods

to the raw sensor data, no additional filtering steps were required during further analysis.

2.4.2 Motion Capture data

The motion capture data was filtered using a third-order Butterworth low-pass filter with a cutoff frequency of 45 Hz. The filtering was performed using the filtfilt method, which applies the filter forwards and backwards to avoid phase distortion. Afther the filtering, the data was resampled using a quadratic interpolation-based resampling method, to 240 Hz.

2.4.3 Force-Plate data

The CoP data was filtered using a third-order Butterworth low-pass filter with a cutoff frequency of 15 Hz. Additionally, the forces from the force plate were filtered using a third-order Butterworth low-pass filter with a cutoff frequency of 45 Hz. Similarly, both filters were applied using the filtfilt method. Values from the force plate lower than 20 N were set to zero. After the filtering process, both the CoP and force-plate data were resampled using a quadratic interpolation-based resampling method to a frequency of 240 Hz.

2.4.4 EMG data

The EMG data was preprocessed in the same way as described in the paper by Gazendam & Hof [30], which means that a 4th-order Butterworth high-pass filter-using a filtfilt method-with a cutoff frequency of 20 Hz was applied first. Subsequently, the data was rectified, and finally, a 4th-order Butterworth low-pass filter with a cutoff frequency of 24 Hz was applied. Afterwards, the data was normalized and resampled using a quadratic interpolation-based resampling method to 240 Hz.
A task-specific normalization method was used, in which the EMG signals were ensemble averaged across all recorded steps at a running speed of 10 km/h. The peak value of this ensemble-averaged EMG waveform served as the normalization reference. A running speed of 10 km/h was chosen for normalization because this pace allowed all participants to run in a relatively natural manner. At higher speeds, the level of training of each participant would have a greater influence, as more trained individuals would require a lower percentage of their maximum muscle strength compared to relatively untrained participants.

2.4.5 Temporal synchronization

The motion capture data and force plate data were recorded using the same software (Qualisys Track Manager, Qualisys AB, Sweden), which ensured that the force plate and motion capture data was already synchronized.
The three jumps at the beginning of each measurement were used to synchronize the motion capture and force plate data with the IMU recordings. Based on Newton's second law, the vertical acceleration of the body's center of mass, approximated by the pelvis acceleration, correlates with the vertical GRF. Therefore, the pelvis acceleration was cross-correlated with the measured vertical GRF to identify the time lag between the two signals. This lag was subsequently used to temporally align the IMU data with the force plate data.
Finally, the EMG signal was synchronized with the IMU data. This was achieved by computing the cross-correlation between the Euclidean norm of the signals from the acceleration sensor connected to the EMG device, mounted directly on top of the IMU sensor on the left upper leg, and the Euclidean norm of the acceleration recorded by that IMU. The cross-correlation was performed over the entire duration of the measurement, and the resulting time lag was used to temporally align the EMG and IMU data.

2.5 Statistical Analysis

Linear Mixed Models (LMMs) were used to analyze the effect of running speed on the peak external and internal force on the tibia, their ratio, peak total TBL, and peak muscle activations. These analyses were performed using the Statsmodels package in Python. The advantage of LMMs is their ability to account for within-participant variability by incorporating random effects.
Separate models were fitted for peak internal force, peak external force, and the ratio of internal to external force as dependent variables, with running speed as a fixed effect predictor. The participant was included as a random intercept to account for inter-individual differences. The model specification was as follows:

$$Y_{i,j} = \beta_0 + \beta_1 \cdot Speed + u_{0,j} + \epsilon_{i,j} \tag{1}$$

Here $Y_{i,j}$ represents the dependent variable (peak internal load, peak external load or ratio) for participant j and speed i. β_0 Is the fixed intercept. β_1 Represents the fixed effect of speed and $u_{0,j}$ is the random intercept for participant j. $\epsilon_{i,j}$ Is the residual error term for speed i and participant j.
Model parameters were estimated using Restricted Maximum Likelihood (REML). Model convergence was assessed. Statistical significance was set at $p < 0.005$. All analyses were performed in the same Python version as used for the Data Processing 2.4 using Statsmodels (v0.14.4).

3 Results

3.1 Tibial Bone Load and Muscle Activations During the Swing and Stance Phases

Figure 3 shows the total TBL, internal muscle force and the external impact force on the tibia during the swing phase and stance phase of the gait cycle, during various running speeds. In addition, muscle activation during these phases are shown for the tibialis anterior, soleus, gastrocnemius medialis and lateralis, during these phases. On average, for 8, 10, 12, 14 km/h, the stance phase took 41.1 ± 4.2%, 38.2 ± 3.2%, 36.2 ± 3.1% and 33.9 ± 2.8% of the gait cycle, respectively.
The internal muscle forces increase proportionally throughout the stance phase at higher speeds. The external impact force mainly increases during the initial peak and between 30% and 80% of the stance phase. The combined increases can be seen in total TBL.
The tibialis anterior is mainly active throughout the swing phase and peaks just before initial contact. During the stance phase the activation is lower and does not increase with speed. The soleus, gastrocnemius medialis and the gastrocnemius lateralis have low activation during the swing phase and are mainly activated just before but mainly during 0% to 80% of the stance phase. Activation patterns of these muscles are similar and increases as running speed increases.
The gastrocnemius lateralis muscle activation shows a rise between 30% and 50% of the swing phase. This is because 2 out of the 9 participants showed activation of this muscle at this moment during the swing. It is suspected that this is related to the generation of ankle stiffness during foot retrieval.

3.2 Effect of Running Speed on Peak Force Magnitudes

Peak values for internal muscle force, external impact force and total TBL increases significantly with an increased running speed (Figure 4). The used LMM, as described

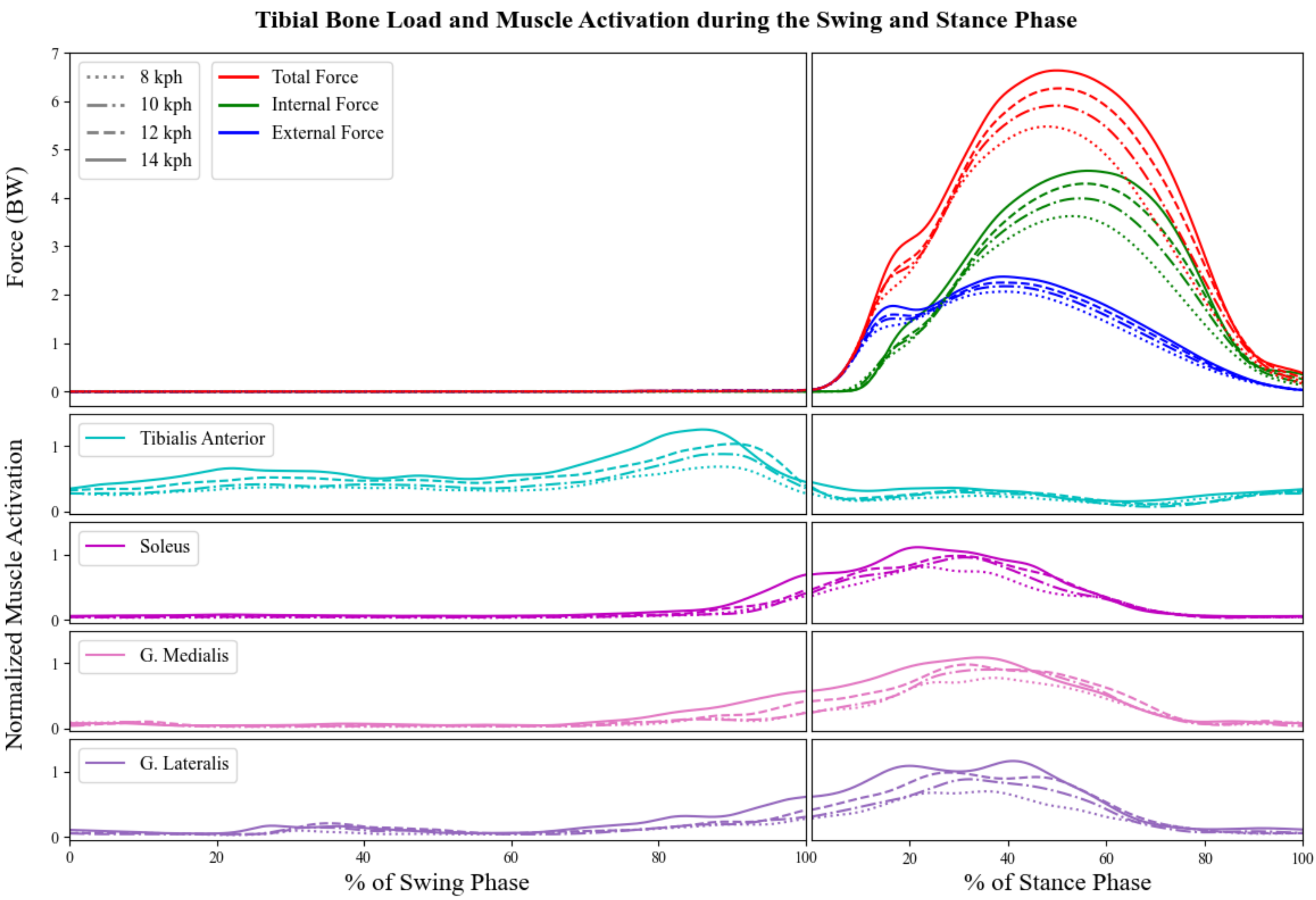

__Figure 3:__ Internal muscle force, external impact force, total TBL, and activations of the tibialis anterior, soleus, gastrocnemius lateralis, and gastrocnemius medialis during the swing and stance phases were assessed across different running speeds and averaged across subjects.

in section 2.5, showed that for every 1 km/h increase in speed, the peak internal muscle force, peak external impact force, and peak total TBL increase by 0.156 ± 0.011 BW, 0.050 ± 0.005 BW, and 0.192 ± 0.016 BW, respectively. The intercepts were 2.43 ± 0.25 BW, 1.67 ± 0.09 BW, and 3.97 ± 0.32 BW for each of these force types. The results were statistically significant ($p < 0.005$ for all forces), indicating a relationship between running speed and peak force magnitudes.

3.3 Ratio of Peak Internal Muscle Forces to External Impact Forces at various Speeds

As can be observed from Figure 5, the ratio between peak internal muscle force and external impact force changes with increasing running speed. This relationship was found to be statistically significant by the described LMM ($p < 0.005$). The ratio increases by 0.028 ± 0.005 for every 1 km/h increase in speed. The estimated intercept was 1.560 ± 0.114.

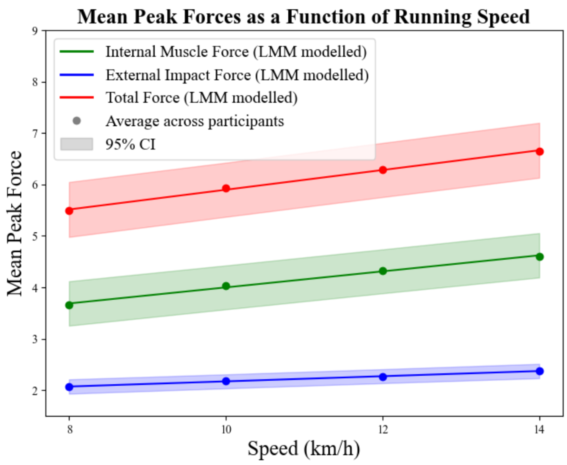

Figure 4: *Mean peak values across subjects for internal muscle force, external impact force, and total TBL at different running speeds. The fitted lines represent predictions from the LMM, with shaded regions indicating 95% confidence intervals.*

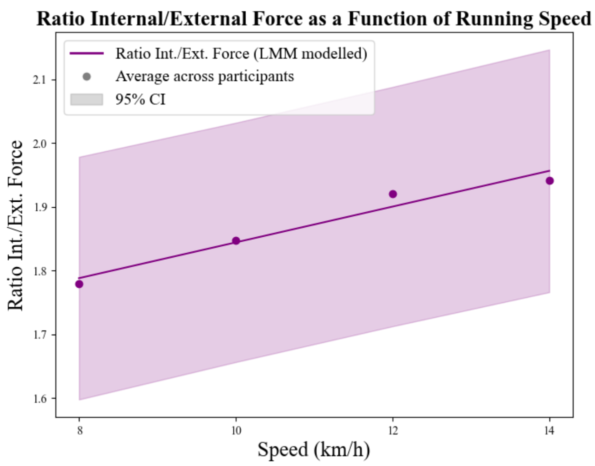

Figure 5: *Mean ratio across subjects at different speeds. The fitted line represents predictions from the LMM, with shaded regions indicating 95% confidence interval.*

3.4 Effect of Running Speed on Peak Muscle Activation Magnitudes

The peak amplitudes in activation of all measured muscles increased significantly with higher speeds, although the rate of increase varied between muscles. The tibialis anterior and gastrocnemius lateralis showed the largest relative increases, with slopes of 0.107 ± 0.011 and 0.101 ± 0.011 per 1 km/h increase in speed, and intercepts of -0.072 ± 0.121 and 0.001 ± 0.13, respectively. In contrast, the soleus and gastrocnemius medialis exhibited smaller increases, with slopes of 0.059 ± 0.008 and 0.041 ± 0.008 per 1 km/h, and intercepts of 0.452 ± 0.101 and 0.596 ± 0.088, respectively. The peak values in relation to running speed for the different muscles are shown in Figure 6.

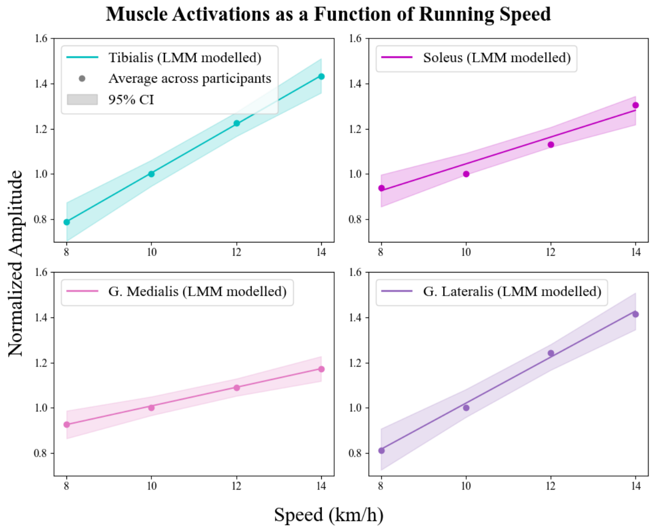

Figure 6: *Mean peak muscle activation values of the tibialis anterior, soleus, gastrocnemius lateralis, and gastrocnemius medialis across subjects at different running speeds. Fitted lines represent predictions from the Linear Mixed Model (LMM), with shaded areas indicating 95% confidence intervals.*

3.5 Timing of Peak Forces and Peak Activations

Running speed had no significant effect on the timing of peak internal muscle forces, external impact forces, or total tibial bone load during the stance phase. The peak internal muscle force occurred at 58.4 ± 0.7% of the stance phase, the peak external impact force at 40.0 ± 0.431%, and the peak total tibial bone load at 52.4 ± 0.523% of the stance phase. Running speed also had no significant effect on the timing of peak muscle activations. The peak activation of the tibialis anterior occurred at 89.2 ± 0.9% of the swing phase, the soleus at 34.8 ± 2.0% of the stance phase, the gastrocnemius medialis at 40.8 ± 1.6% of the stance phase, and the gastrocnemius lateralis at 36.9 ± 1.8% of the stance phase.

4 Discussion

This research aimed to investigate the effect of running speed on the total TBL, the internal muscle and external impact components, and the dynamics of muscle activation. Both internal muscle forces, external impact forces, and the total TBL significantly increase as speed increases. This finding is consistent with the limited research available in this field [37, 38]. The peak values for internal muscle forces increase relatively more than the peak external impact forces, leading to an increase in the ratio between these two components of the TBL as speed increases. Speed had no effect on when during the stance phase the peak internal muscle force, external impact force, or total TBL occurred, meaning that the moment of peak loading on the tibia remains unchanged across speeds.

The values for internal muscle forces, and consequently total tibial bone loading (TBL), were slightly lower but within the same order of magnitude as those reported by Matijevich et al. (2019) and Zandbergen et al. (2023), who used comparable modeling approaches [21, 22]. In this study, a peak internal muscle force of 4.3 ± 0.7 BW was observed at a running speed of 12 km/h, compared to 5.5 BW (Matijevich et al., 2019) and 5.3 ± 0.6 BW (Zandbergen et al., 2023) [21, 22]. In contrast, the external impact forces observed in this study (2.3 ± 0.2 BW) were well aligned with those reported in the same studies (2.0 and 2.4 ± 0.2 BW, respectively)[21, 22]. This resulted in a total TBL of 6.3 ± 0.8 BW, which is slightly lower than the 7.5 BW and 7.6 ± 0.6 BW reported by Matijevich et al. (2019) and Zandbergen et al. (2023), respectively [21, 22]. GRFs, external impact forces, and the Achilles tendon moment arm used in the current study were consistent with the values reported in these studies. Therefore, the observed difference in peak internal muscle force may be attributed to a variation in ankle moment arm. Specifically, the anterior–posterior distance between the CoP and the ankle joint center. Each study employed a different method to estimate the ankle joint position, which directly affects the calculated moment arm and thus the internal muscle force.

In the study by Matijevich et al. (2019), the functional ankle joint position was determined from markers on the lower limbs, and calculated using C-Motion Visual3D software [21]. Zandbergen et al. (2023), used a novel method to spatially align force plate and inertial measurement unit data by using the center of pressure crossing a virtual toe marker to estimate the ankle moment arm [22]. This approach relies on more assumptions and estimations compared to the approach used in the present study, in which the ankle position was derived directly from a marker placed on the medial malleolus. As a result, the outcomes of the current study are likely to be more reliable.

It was assumed that the functional axis of rotation of the ankle coincides with the center of the medial malleolus. This assumption is justified because the midpoint between the medial and lateral malleolus lies only around 16 mm from the functional axis of rotation, and the medial malleolus is positioned more anteriorly than the lateral malleolus, which helps to counteract this small offset [39]. A difference in ankle joint position between studies may be a plausible explanation for the observed discrepancies in reported values. To illustrate the impact of small variations in the vertical position of the functional ankle joint axis in the sagittal plane, the effects of different vertical joint offsets were calculated and are presented in Table 1.

Table 1: *Peak internal muscle forces, external impact forces, and total TBL for different ankle offsets.*

Offset	-20 mm	-10 mm	0 mm	10 mm	20 mm
$F_{\text{int}}(BW)$	5.2 ± 0.7	4.8 ± 0.7	4.3 ± 0.7	3.9 ± 0.6	3.5 ± 0.6
$F_{\text{ext}}(BW)$	2.4 ± 0.2	2.4 ± 0.2	2.4 ± 0.2	2.4 ± 0.2	2.4 ± 0.2
$F_{\text{total}}(BW)$	7.2 ± 0.9	6.7 ± 0.9	6.3 ± 0.8	5.8 ± 0.8	5.4 ± 0.8

Minor offsets were found to have a substantial impact on the estimated internal muscle forces. Approximately -0.4 times BW per 10 mm offset. This sensitivity highlights how slight differences in joint center estimation may account for the notable variation between values reported in the literature and those observed in the current study. To estimate internal muscle forces, only the vertical component of the GRF was used, rather than the full GRF vector in the sagittal plane. This choice was made because the anterior-posterior GRF component is relatively small and oscillates around zero. As a result, it has a negligible effect on the total GRF magnitude. Especially after squaring the components during vector calculation. In balancing model complexity and clarity, the anterior-posterior component was therefore excluded to maintain a simpler and more interpretable model.

The muscle activation patterns in this study show the same patterns as presented in literature [30, 40]. where the tibialis anterior is especially active during the swing phases and shows a peak just before initial contact (Figure 3). The activation patterns of the soleus, gastrocnemius medialis, and gastrocnemius lateralis are similar, showing a single burst that begins just before initial contact and is primarily present during the first 80% of the stance phase (Figure 3). What is striking about the activation patterns over the swing and stance phases is that the tibialis anterior shows higher values during the entire swing phase, and especially during the peak just before initial contact. The higher peak value during the swing phase is due to the fact that, at higher speeds, the foot experiences greater translational acceleration [41]. As a result, the tibialis anterior must generate a larger moment to overcome the inertia of the foot segment and properly position the foot for initial contact. This effect is particularly evident at the point of maximum dorsiflexion, just before initial contact [42]. The influence of running speed on the activation patterns of the soleus, gastrocnemius medialis, and gastrocnemius lateralis is also similar across these muscles. Increased velocity leads to a comparable rise in activation throughout the entire peak duration.

During the stance phase, the tibialis anterior is also active, but to a lesser degree, and it undergoes an eccentric contraction. During this phase, the tibialis anterior also shows a low mid-stance peak. Although the mid-stance peak is relatively low and does not increase substantially as can be seen in Figure 1, it does increase significantly as speed increases, according to the performed LMM ($p < 0.005$). For every 1 km/h increase in speed, the peak increases by 0.024 ± 0.004. This gives us the indication that co-contraction slightly increases with speed. However, it is important to note that eccentric and concentric contractions may have different effects on the EMG signal

[43, 44].

The task-specific normalization method used in this study has both advantages and disadvantages compared to the commonly used MVC method. One advantage is that the used method reduces inter-subject variability, making it easier to compare participants [45]. It also offers a practical benefit, as no time-consuming MVC protocol had to be performed before the measurements. On the other hand, interpreting the data is generally more straightforward with MVC normalization, as activation can then be expressed as a percentage of maximal contraction (0–100% MVC).

The sagittal plane ankle model, used in this study to model the forces on the tibia, has several limitations [22, 29, 23]. Firstly, the model is only suitable for estimating the load on the tibia during the stance phase, while during the swing phase, muscle forces also act on the tibia, as can be seen in Figure 1. Additionally, it assumes that the mass and inertia of the foot are negligible, and because of the use of the net ankle moment, the model does not account for co-contraction. Nevertheless, it is assumed that the model still provides a good approximation of the forces acting on the bone [22, 29]. Since the increases in tibialis activation during mid stance are relatively small, the model is not expected to deviate significantly from the actual forces at higher speeds.

Additionally, the model assumes that the tibia behaves as a rigid segment, while in reality, it undergoes slight bending [22, 46]. During running, this bending generates additional shear forces within the bone tissue that are not captured by the model [22, 46]. The bending-induced stresses reported in literature and the compression forces acting on the bone, as estimated in this study, increase in a similar proportion with increasing running speed [38]. As a result, the compression forces calculated in this study can still be a good measure of the degree of loading.

In this study, TBL is used as a measure of the load on the tibia. In reality, this load is distributed between the tibia and the fibula, which is positioned parallel to the tibia. Studies have shown that the fibula carries approximately 10% of the total axial load [47, 48]. Therefore, the actual forces acting solely on the tibia are slightly lower than the reported TBL. It is assumed that this distribution remains relatively constant with increasing running speed, as overall running kinetics do not change significantly with increasing running speed [49].

Although this study focuses primarily on load per step, it is particularly relevant for practice to understand how repeated steps, and thus cumulative load, contribute to the development of injuries. An increase in running speed involves fewer steps per kilometer, but in a larger loading per step. While Hunter et al. (2019) reported a decrease in cumulative tibial load per distance as speed increases, van Hooren et al. (2024) found no significant difference in cumulative tibial loads. [37, 38]

It is questionable whether current methods of calculating cumulative load do sufficient justice to the complexity of overuse injuries. The high standard deviation in load measures between subjects in those studies suggests that there can be a great difference between runners [37, 38]. The large differences between individuals show that this relationship can be different for each individual.

In this context, the ratio of internal muscle forces to external impact forces examined in this study, combined with a minimal sensor configuration in which external forces can be estimated, offers an interesting opportunity to do future studies in the field. This approach could enable an accessible way to assess runner specific tibial loading in the future, without placing significant demands on the runner. In this way, it would be possible in the future to set up a prospective cohort study. In such a study, runners could be followed over a longer period of time to investigate which cumulative loading measures are the strongest predictors of overuse-related injuries.

5 Conclusion

This study aimed to investigate the effect of running speed on tibial loading, as well as the effect of speed on muscle activation of the tibialis anterior, soleus, gastrocnemius medialis, and gastrocnemius lateralis during both the stance and swing phase.

The results show that internal muscle forces, external impact forces, and total TBL all increase significantly with running speed. The increase in peak internal muscle forces was greater than that of the external impact forces, indicating that the ratio between these forces increases as running speed increases. Speed did not significantly affect the timing of the peak forces.

The tibialis anterior was primarily active during the swing phase and showed increased muscle activation throughout this phase as speed increased, particularly just before initial contact. The soleus, gastrocnemius medialis, and gastrocnemius lateralis showed similar muscle activation patterns, with peaks beginning just before initial contact and ending around 80% into the stance phase. The tibialis anterior and gastrocnemius lateralis exhibited the largest relative increase in peak muscle activation.

This study focused on loading per individual step, rather than cumulative load over time. The ratios between peak internal muscle forces and external impact forces may be useful, in combination with additional sensor data, for estimating total tibial loading in a practical and accessible manner.

This may open the door for future prospective studies that investigate which specific load-related parameters are most strongly associated with the development of overuse injuries. By identifying these predictors, researchers can gain a better understanding of how individual loading patterns contribute to injury risk. This knowledge can in turn be used to design more personalized and targeted training or rehabilitation strategies, aimed at reducing the likelihood of injury and improving long-term running performance and safety.

6 Acknowledgements

First of all, I want to sincerely thank my supervisor, Dr. J. Reenalda, for his invaluable guidance, thoughtful advice, insightful perspective, and enjoyable conversations. His support has been crucial in helping me create a piece of work I'm truly proud of and have learned a great deal from.

I would also like to express my gratitude to the other members of my examination committee, Dr. Ir. B. L. Scheltinga and Prof. Dr. Ir. M. Sartori, for their expertise, constructive feedback, and valuable insights. Their contributions have significantly enhanced the quality of my research.

Furthermore, I am grateful to the technical staff of the Biomedical Signals & Systems and Biomechanical Engineering research groups at the University of Twente, as well as to the participants who generously took part in the experiments and helped make data collection possible.

I also want to thank the IMMUnity team, where an impressive amount of knowledge was shared, enabling me to overcome numerous challenges and successfully carry out my experiments.

Finally, I want to thank my family and friends for their continuous interest, good advice, patience, and for asking thousands of times whether I was almost finished with my master's research. To them, I say: almost!

Lastly, I would like to acknowledge the assistance of AI-based language tools in enhancing the clarity and readability of this thesis.

References

1. Lavie CJ, Lee Dc, Sui X, Arena R, O'Keefe JH, Church TS, Milani RV, and Blair SN. Effects of Running on Chronic Diseases and Cardiovascular and All-Cause Mortality. Mayo Clinic Proceedings 2015 Nov; 90:1541–52. DOI: 10.1016/j.mayocp.2015.08.001
2. Gent RN van, Siem D, Middelkoop M van, Os AG van, Bierma-Zeinstra SMA, Koes BW, and Taunton JE. Incidence and determinants of lower extremity running injuries in long distance runners: a systematic review * COMMENTARY. British Journal of Sports Medicine 2007 Mar; 41:469–80. DOI: 10.1136/bjsm.2006.033548
3. Kluitenberg B, Middelkoop M van, Diercks R, and Worp H van der. What are the Differences in Injury Proportions Between Different Populations of Runners? A Systematic Review and Meta-Analysis. Sports Medicine 2015 Aug; 45:1143–61. DOI: 10.1007/s40279-015-0331-x
4. James SL, Bates BT, and Osternig LR. Injuries to runners. The American Journal of Sports Medicine 1978 Mar; 6:40–50. DOI: 10.1177/036354657800600202
5. McBryde AM. Stress Fractures in Runners. Clinics in Sports Medicine 1985 Oct; 4:737–52. DOI: 10.1016/S0278-5919(20)31190-X
6. Milgrom C. Do high impact exercises produce higher tibial strains than running? British Journal of Sports Medicine 2000 Jun; 34:195–9. DOI: 10.1136/bjsm.34.3.195
7. Matheson G, Clement D, Mckenzie D, Taunton J, Lloyd-Smith D, and Macintyre J. Stress fractures in athletes. The American Journal of Sports Medicine 1987 Jan; 15:46–58. DOI: 10.1177/036354658701500107
8. Hoenig T, Ackerman KE, Beck BR, Bouxsein ML, Burr DB, Hollander K, Popp KL, Rolvien T, Tenforde AS, and Warden SJ. Bone stress injuries. Nature Reviews Disease Primers 2022 Apr; 8:26. DOI: 10.1038/s41572-022-00352-y
9. Romani WA, Gieck JH, Perrin DH, Saliba EN, and Kahler DM. Mechanisms and management of stress fractures in physically active persons. Journal of athletic training 2002 Jul; 37:306–14
10. Brukner PM, Bradshaw CM, Khan KMM, White SM, and Crossley KB. Stress Fractures: A Review of 180 Cases. Clinical Journal of Sport Medicine 1996 Apr; 6:85–9
11. Hulkko A and Orava S. Stress Fractures in Athletes. International Journal of Sports Medicine 1987 Jun; 08:221–6. DOI: 10.1055/s-2008-1025659
12. Bennell K, Matheson G, Meeuwisse W, and Brukner P. Risk Factors for Stress Fractures. Sports Medicine 1999; 28:91–122. DOI: 10.2165/00007256-199928020-00004
13. Xiang L, Gao Z, Wang A, Shim V, Fekete G, Gu Y, and Fernandez J. Rethinking running biomechanics: a critical review of ground reaction forces, tibial bone loading, and the role of wearable sensors. Frontiers in Bioengineering and Biotechnology 2024 Apr; 12. DOI: 10.3389/fbioe.2024.1377383
14. Lanyon LE, Hampson WGJ, Goodship AE, and Shah JS. Bone Deformation Recorded in vivo from Strain Gauges Attached to the Human Tibial Shaft. Acta Orthopaedica Scandinavica 1975 Jan; 46:256–68. DOI: 10.3109/17453677508989216
15. Komi PV. Relevance of in vivo force measurements to human biomechanics. Journal of Biomechanics 1990 Jan; 23:23–34. DOI: 10.1016/0021-9290(90)90038-5
16. Worp H van der, Vrielink JW, and Bredeweg SW. Do runners who suffer injuries have higher vertical ground reaction forces than those who remain injury-free? A systematic review and meta-analysis. British Journal of Sports Medicine 2016 Apr; 50:450–7. DOI: 10.1136/bjsports-2015-094924
17. Johnson CD, Tenforde AS, Outerleys J, Reilly J, and Davis IS. Impact-Related Ground Reaction Forces Are More Strongly Associated With Some Running Injuries Than Others. The American Journal of Sports Medicine 2020 Oct; 48:3072–80. DOI: 10.1177/0363546520950731
18. Tenforde AS, Hayano T, Jamison ST, Outerleys J, and Davis IS. Tibial Acceleration Measured from Wearable Sensors Is Associated with Loading Rates in Injured Runners. PM&R 2020 Jul; 12:679–84. DOI: 10.1002/pmrj.12275
19. Burke A, Dillon S, O'Connor S, Whyte EF, Gore S, and Moran KA. Comparison of impact accelerations between injury-resistant and recently injured recreational runners. PLOS ONE 2022 Sep; 17:e0273716. DOI: 10.1371/journal.pone.0273716
20. Zhang JH, An WW, Au IP, Chen TL, and Cheung RT. Comparison of the correlations between impact loading rates and peak accelerations measured at two different body sites: Intra- and inter-subject analysis. Gait & Posture 2016 May; 46:53–6. DOI: 10.1016/j.gaitpost.2016.02.002
21. Matijevich ES, Branscombe LM, Scott LR, and Zelik KE. Ground reaction force metrics are not strongly correlated with tibial bone load when running across speeds and slopes: Implications for science, sport and wearable tech. PLOS ONE 2019 Jan; 14:e0210000. DOI: 10.1371/journal.pone.0210000

22. Zandbergen MA, Ter Wengel XJ, Middelaar RP van, Buurke JH, Veltink PH, and Reenalda J. Peak tibial acceleration should not be used as indicator of tibial bone loading during running. Sports Biomechanics 2023 Jan :1–18. DOI: 10.1080/14763141.2022.2164345
23. SCOTT SH and WINTER DA. Internal forces at chronic running injury sites. Medicine & Science in Sports & Exercise 1990 Jun; 22:357???369. DOI: 10.1249/00005768-199006000-00013
24. Winter DA and Bishop PJ. Lower Extremity Injury. Sports Medicine 1992 Sep; 14:149–56. DOI: 10.2165/00007256-199214030-00001
25. Sasimontonkul S, Bay BK, and Pavol MJ. Bone contact forces on the distal tibia during the stance phase of running. Journal of Biomechanics 2007; 40:3503–9. DOI: 10.1016/j.jbiomech.2007.05.024
26. Brockett CL and Chapman GJ. Biomechanics of the ankle. Orthopaedics and Trauma 2016 Jun; 30:232–8. DOI: 10.1016/j.mporth.2016.04.015
27. Cohen JC. Anatomy and Biomechanical Aspects of the Gastrocsoleus Complex. Foot and Ankle Clinics 2009 Dec; 14:617–26. DOI: 10.1016/j.fcl.2009.08.006
28. Semple R, Murley GS, Woodburn J, and Turner DE. Tibialis posterior in health and disease: a review of structure and function with specific reference to electromyographic studies. Journal of Foot and Ankle Research 2009 Jan; 2. DOI: 10.1186/1757-1146-2-24
29. Matijevich ES, Scott LR, Volgyesi P, Derry KH, and Zelik KE. Combining wearable sensor signals, machine learning and biomechanics to estimate tibial bone force and damage during running. Human Movement Science 2020 Dec; 74:102690. DOI: 10.1016/j.humov.2020.102690
30. Gazendam MG and Hof AL. Averaged EMG profiles in jogging and running at different speeds. Gait & Posture 2007 Apr; 25:604–14. DOI: 10.1016/j.gaitpost.2006.06.013
31. Kernozek T, Gheidi N, and Ragan R. Comparison of estimates of Achilles tendon loading from inverse dynamics and inverse dynamics-based static optimisation during running. Journal of Sports Sciences 2017 Nov; 35:2073–9. DOI: 10.1080/02640414.2016.1255769
32. Benson LC, Clermont CA, Bošnjak E, and Ferber R. The use of wearable devices for walking and running gait analysis outside of the lab: A systematic review. Gait & Posture 2018 Jun; 63:124–38. DOI: 10.1016/j.gaitpost.2018.04.047
33. Caldas R, Mundt M, Potthast W, Buarque de Lima Neto F, and Markert B. A systematic review of gait analysis methods based on inertial sensors and adaptive algorithms. Gait & Posture 2017 Sep; 57:204–10. DOI: 10.1016/j.gaitpost.2017.06.019
34. Scheltinga BL, Kok JN, Buurke JH, and Reenalda J. Estimating 3D ground reaction forces in running using three inertial measurement units. Frontiers in sports and active living 2023; 5:1176466. DOI: 10.3389/fspor.2023.1176466
35. Mayne RS, Bleakley CM, and Matthews M. Use of monitoring technology and injury incidence among recreational runners: a cross-sectional study. BMC Sports Science, Medicine and Rehabilitation 2021 Dec; 13:116. DOI: 10.1186/s13102-021-00347-4
36. Stegeman D and Hermens H. Standards for suface electromyography: The European project Surface EMG for non-invasive assessment of muscles (SENIAM). 2007 Mar; 1
37. HUNTER JG, GARCIA GL, SHIM JK, and MILLER RH. Fast Running Does Not Contribute More to Cumulative Load than Slow Running. Medicine & Science in Sports & Exercise 2019 Jun; 51:1178–85. DOI: 10.1249/MSS.0000000000001888
38. Van Hooren B, Rengs L van, and Meijer K. Per-step and cumulative load at three common running injury locations: The effect of speed, surface gradient, and cadence. Scandinavian Journal of Medicine & Science in Sports 2024 Feb; 34. DOI: 10.1111/sms.14570
39. Sado N, Shiotani H, Saeki J, and Kawakami Y. Positional difference of malleoli-midpoint from three-dimensional geometric centre of rotation of ankle and its effect on ankle joint kinetics. Gait & Posture 2021 Jan; 83:223–9. DOI: 10.1016/j.gaitpost.2020.10.018
40. Darendeli A, Ertan H, Cuğ M, Wikstrom E, and Enoka RM. Comparison of EMG activity in shank muscles between individuals with and without chronic ankle instability when running on a treadmill. Journal of Electromyography and Kinesiology 2023 Jun; 70:102773. DOI: 10.1016/j.jelekin.2023.102773
41. Lafortune MA. Three-dimensional acceleration of the tibia during walking and running. Journal of Biomechanics 1991 Jan; 24:877–86. DOI: 10.1016/0021-9290(91)90166-K
42. CHAN CW and RUDINS A. Foot Biomechanics During Walking and Running. Mayo Clinic Proceedings 1994 May; 69:448–61. DOI: 10.1016/S0025-6196(12)61642-5
43. Mchugh MP, Tyler TF, Greenberg SC, and Gleim GW. Differences in activation patterns between eccentric and concentric quadriceps contractions. Journal of Sports Sciences 2002 Jan; 20:83–91. DOI: 10.1080/026404102317200792
44. Madeleine P, Bajaj P, Søgaard K, and Arendt-Nielsen L. Mechanomyography and electromyography force relationships during concentric, isometric and eccentric contractions. Journal of Electromyography and Kinesiology 2001 Apr; 11:113–21. DOI: 10.1016/S1050-6411(00)00044-4
45. Burden A, Trew M, and Baltzopoulos V. Normalisation of gait EMGs: a re-examination. Journal of Electromyography and Kinesiology 2003 Dec; 13:519–32. DOI: 10.1016/S1050-6411(03)00082-8
46. Yang PF, Sanno M, Ganse B, Koy T, Brüggemann GP, Müller LP, and Rittweger J. Torsion and Antero-Posterior Bending in the In Vivo Human Tibia Loading Regimes during Walking and Running. PLoS ONE 2014 Apr; 9:e94525. DOI: 10.1371/journal.pone.0094525
47. Calhoun JH, Li F, Ledbetter BR, and Viegas SF. A Comprehensive Study of Pressure Distribution in the Ankle Joint with Inversion and Eversion. Foot & Ankle International 1994 Mar; 15:125–33. DOI: 10.1177/107110079401500307
48. FUNK JR, RUDD RW, KERRIGAN JR, and CRANDALL JR. The Effect of Tibial Curvature and Fibular Loading on the Tibia Index. Traffic Injury Prevention 2004 Jun; 5:164–72. DOI: 10.1080/15389580490436069

49. Brughelli M, Cronin J, and Chaouachi A. Effects of Running Velocity on Running Kinetics and Kinematics. Journal of Strength and Conditioning Research 2011 Apr; 25:933–9. DOI: 10.1519/JSC.0b013e3181c64308